Bulg. J. Phys. 29 (2002) 17–29

FABRICATION OF DIFFRACTION GRATINGS FOR MICROFLUIDIC ANALYSIS

Y. SAROV
Central Laboratory of Optical Storage and Processing of Information
Bulgarian Academy of Sciences
P.O. Box 95, 1113 Sofia, Bulgaria

I. KOSTIC, P. HRKUT, L. MATAY
Institute of Informatics, Slovak Academy of Sciences,
9 Dubravska cesta Str., SK-842 37 Bratislava, Slovakia

TZ. IVANOV, I. RANGELOW
Institute of Technological Physics, IMA, University of Kassel
FB-18, Heinrich-Plett Str. 40, D-34132 Kassel, Germany

Abstract. Micro-optical-electromechanical systems for microfluidic applications include typically different constituents, as optical fibers, waveguides, wavelength selection gratings and microfluidic parts, all on a single chip. In this work high quality micrometer-period metal and submicrometer silicon diffraction gratings are fabricated by e-beam lithography and reactive ion etching. Fabricated gratings' quality and optical behaviour is investigated. Sub-micrometer period diffraction gratings can be used as high selective optical grids in the visible region, as well as diffractive grids in UV and X-ray regions. Examples of obtained 2D and 3D diffraction structures are presented.

PACS number: 42.79.Dj, 42.82. Cr, 42.62.Be

1. Introduction

Micro-optical-electromechanical systems technology opens the possibility to obtain remote, highly accurate measurements and sensing. Total Internal Reflection (TIR) phenomenon, in combination with diffraction of light from a grating, can be used for development of high sensitive reflectometric and re-

1310–0157 © 2002 Heron Press Ltd.

fractometric devices for investigation and analysis of liquids. In such sensors the material, quality, thickness and period of grating define the orders' energy distribution, as well as the angular and spectral selectivity, while the preparation method determines possibilities of the grating integration in the sensor's chip during the fabrication.

An important example of fluidic analysing system is a Diffraction Grating (DG), working in TIR mode and contacting the fluid under investigation. TIR-DG is applied in sensors for transparent and absorbing liquids investigation [1–4] and has shown strong sensitivity both to the real (i.e. the refractive index) and the imaginary (i. e. absorption coefficient) parts of square root of the dielectric permittivity. Another DG application in liquids optical investigation is related with the microrefractometer, described in [5, 6]. In the device a binary metal DG is used to indicate the TIR occurrence by the diffraction pattern disappearance. Precise measurement of the sample's refractive index, led by the refractometer, can be used to determine the fluid composition and evaluation of the components' concentration [7].

Techniques as mechanical process [9], lithography [10, 12], holography [13, 14], etching [15, 16] and the combination between them [13, 17] are usually employed for DGs fabrication. In case of small number of diffraction structures with user specified geometry, e-beam direct writing combines excellent flexibility in structures shape formation with large depth of focus and high resolution in case of pattering non-planar surfaces. The throughput is substantially increased in the case of vector scanning mode of the e-beam and variable shot shape [18]. Another advantage of the e-beam lithography is its compatibility with the developed silicon chips production technologies.

The goal of this work is to present fabrication of DSs, used in the development of microsensors and microdevices for detecting biological and chemical agents. Such devices can be applied in numerous fields, including biocompatible materials engineering, biomolecule separation, controlled drug delivery and bioanalytical sensing [8]. Gratings with different periods and geometry are prepared by e-beam lithography and Reactive Ion Etching (RIE). Optical behavior of the metal gratings is investigated in planar geometry as well as in TIR mode. Examples of obtained 2D and 3D diffraction structures are shown.

2. Experimental and Results

2.1. Fabrication of Metal DGs

A high quality Hoya 3″ glass substrate with Cr layer of thickness $t = 95$ nm is used for metal gratings preparation. The metal layer is covered with 500 nm negative e-beam resist NS-125. Direct e-beam exposure is performed at 30 keV by pattern generator-modified ZBA 10/1 e-beam lithography system, made in

Carl Zeiss Jena. The lithograph uses vector scan mode and has variable shape rectangular shot, which substantially increases the speed of the writing process. The e-beam current density is kept constant at 0.4 A/cm^2. A suitable exposure dose is chosen by varying the single shot duration τ. Under the described conditions the optimal single shot exposure time of 25 μs is experimentally determined. After exposure the resist is developed and Cr wet etching for 90 s is performed in mixture of $Ce(NH_4)_2(NO_3)_6$ and $HClO_4$ in distilled water. Finally, the resist is striped in mixture of 2-ethoxyethyl-acetate and xylene.

Eight linear DGs are exposed on one substrate. It is cut by diamond saw to separate the elements. Microscopic pictures of some of the gratings at different magnification are shown in Fig. 1*a*, *c*, *d*. The metal DGs are designed with long $p = 34.5$ and short $3q = 4.5$ mm grating side in two general configurations — with lines transversal (Fig. 1*a*) and longitudinal (Fig. 1*c*, *d*) according to the longer side of the grating area. The range of the gratings' geometrical parameters are: metal line width $d = 3.5..10$ μm, period $\Lambda = 6..20$ μm, filling factor $\xi = 0.35..0.58$ (defined as line width to period ratio) and spatial frequency $f = 1/\Lambda = 50..167$ lines/mm. Excellent line quality can be reported since the line roughness and the average defects size is estimated of about 200..300 nm.

The linear DGs with transversal lines are typical for batch produced linear gratings. The DGs from the second type (with longitudinal lines) have been proposed to be applied as optical as well as thermo-sensitive elements. For this purpose the chromium lines connect electrically four contact areas ($1.5\times$ 1.5 mm), situated in the corners of the grating, as is shown schematically in Fig. 1*b*. The lines in the left third part finished 0.1 mm before the lower left contact thus the left pair electrodes is connected only by one metal line. The corresponding resistance R_1 is:

$$R_1 = R_\square \frac{p - 2q}{d} \sim R_\square \frac{p}{d}$$

where $R_\square$ is the Cr layer sheet resistance. Lines in the middle part are connected consequently in meander shape thus the resistance between the upper pair electrodes R_2 is

$$R_2 = R_\square \frac{fq}{d}\left[p + \xi(\Lambda - d)\right] \sim R_1 fq\,.$$

Resistance R_3 between the right contact pair, where lines are parallel connected is

$$R_3 = R_\square \frac{p - 2q}{fqd} \sim \frac{R_1}{fq}\,.$$

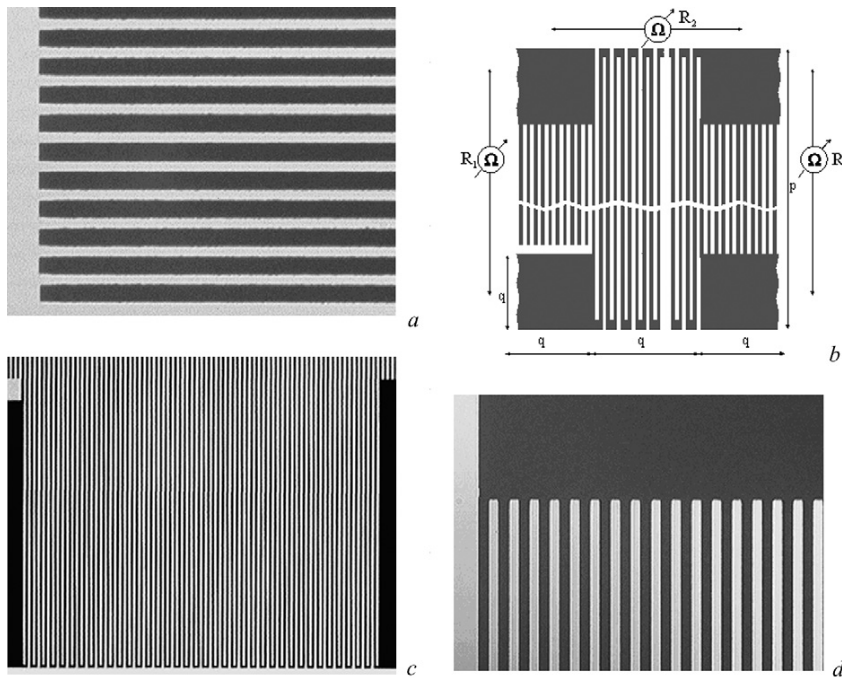

Fig. 1. Chromium diffraction gratings
(*a*) DG with $d = 3.5\ \mu$m and $\Lambda = 6\ \mu$m (transversal lines); (*b*) design of the DGs with longitudinal lines; (*c*) DG with $d = 10\ \mu$m and $\Lambda = 20\ \mu$m (longitudinal lines); (*d*) DG with $d = 5\ \mu$m and $\Lambda = 10\ \mu$m (longitudinal lines)

Thin copper wires are attached to the contact pads by indium solders at 250 °C. The resistance between electrodes is measured by digital multimeter Tektronix DM. The values of R_1, R_2 and R_3 for different gratings are in the range of 70..200 kΩ, 6..32 MΩ and 1.0..1.6 kΩ, respectively. Since in our geometry fq is between 75 and 167 there are choices of resistance values distinguished in four orders of magnitude. Thus a proper pair can be chosen for measurement with maximum accuracy, which depends on the measuring instrument type and technique, the current value in the electrical circuit, etc. Sheet resistance value for the Cr layer is calculated of $R_\square = 22.6 \pm 0.1\ \Omega$. The temperature coefficient of resistance, equal to $4{\times}10^{-4}$ K^{-1}, is determined in the temperature range 0..25 °C. This value is smaller than the typical for the bulk chromium value $6{\times}10^{-3}$ K^{-1}. The difference could be explained by existence of particular electrical connected Cr islands in a matrix of insulating chromium oxide areas in the film, affecting in increase in the layer's specific resistance and decrease in resistance temperature coefficient [19].

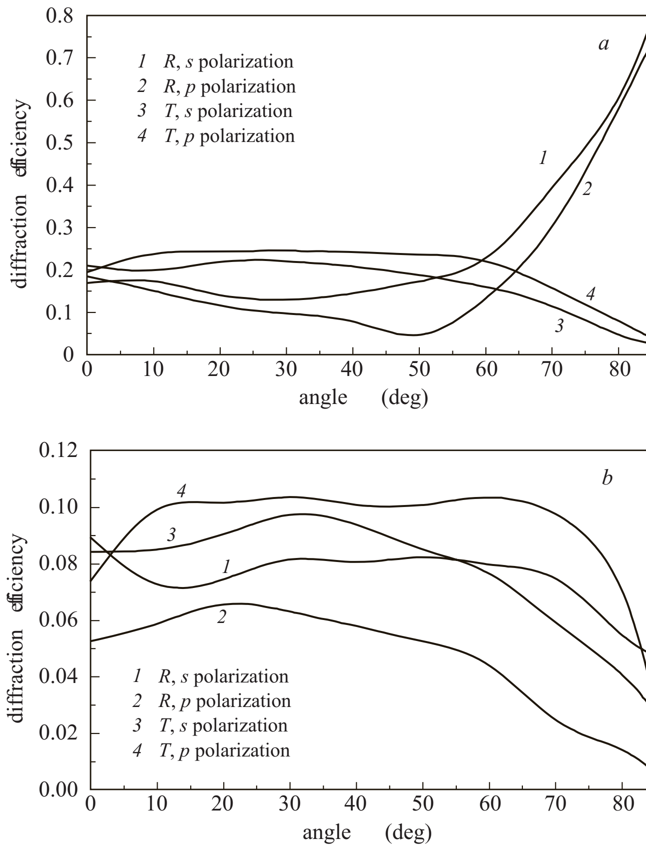

Fig. 2. DE angular dependence in reflection and transmission (a) 0-th order; (b) -1-st order. In the graphs *1* and *2* correspond to reflection, s and p polarization, respectively, *3* and *4* — to transmission, s and p polarization, respectively

Diffraction efficiencies (DEs) of the DGs are investigated in planar configuration, where the DGs are directly illuminated. A He–Ne laser light with wavelength $\lambda = 633$ nm is used as a light source. Both reflection and transmission orders are investigated at different angles of incidence q and for polarization of light with electrical vector perpendicular (s) and parallel (p) to the plane of incidence. Although up to ± 17 order could be visually distinguished, more than 60 % of the energy is concentrated in 0-th and ± 1 transmitted and reflected orders (minus numbered orders propagates closer to normal incidence direction). Figure 2 illustrates the angular dependence of the measured DEs —

η_0 of the 0-th and η_1 of the -1 orders for the case of a grating with $d = 5\,\mu$m and $\Lambda = 10\,\mu$m. The investigation of the other prepared gratings shows that the orders DE behaviour are similar and only the summary energy distribution between the reflected and transmitted light is changed proportionally with the filling factor ξ. Many diffraction orders existence and relatively low DE are typical for thin amplitude gratings working in Raman–Nath regime [20].

Other important application of the thin metal DGs is possible in TIR mode. In such configuration the grating is situated between two media with different refractive indices and illuminated from the optically denser medium at angles of incidence, larger than the critical angle. The experimental results show that the metal DGs' optical behaviour is similar to that of pure phase gratings. The orders' DEs are few times greater [21] than in planar geometry and are strongly sensitive both to the real (i. e. the refractive index) and imaginary (i. e. absorption coefficient) parts of square root of the relative dielectric permittivity $\sqrt{\varepsilon}$ [1–4].

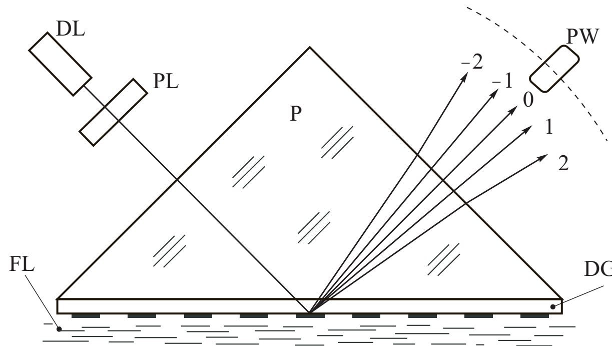

Fig. 3. Operation principle of TIRDG based reflectometer for microfluidic analytical application
DL diode laser, P prism, DG diffraction grating, PL polarizer, PW powermeter, FL fluid under investigation

Experimentally the grating (DG) is pasted to a glass prism (P) with the substrate toward with the help of index matching liquid (Fig. 3). The prism has been chosen, made from glass K8 with refractive index 1.515, close to that of the substrate. The grating's metal lines are in contact with the fluid (FL) under investigation. The experiments are led with the radiation from a diode laser (DL), emitting at 633 nm. Orders DEs are measured in reflection by a powermeter (PW). The polarizer (PL) chooses the proper light polarization. Measurements of the orders' DE polarization and angular dependence are led for water as a rarer medium (for detailed investigation of the TIR-DG's sensitivity

according to the fluid's optical constant e. g. [1–2]). Results are presented in Fig. 4*a*, *b*. In vicinity of the critical angle, equal to 61.5°, specific behaviour of the orders could be observed. The 0-th order shows maximum DE in case of p polarization while the ± 1 orders undergo minimum. Opposite case happens for the orthogonal polarization: 0-th order has minimum and ± 1 orders — maximum. These peculiarities could be explained as a result of the energy redistribution during the transformation of the propagating transmitted orders into evanescent ones at the critical angle.

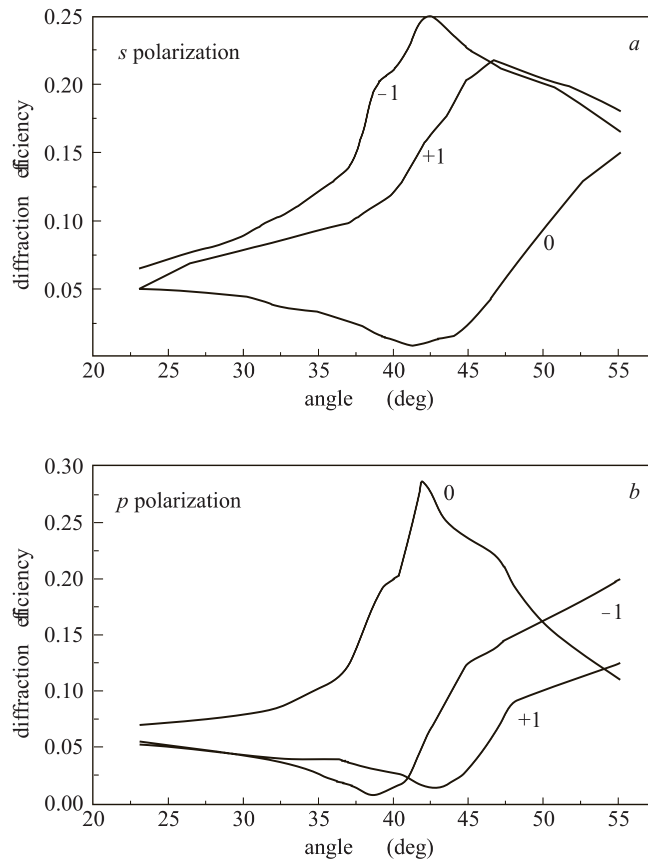

Fig. 4. DE angular dependence of the 0-th and ± 1-st order in the case of TIRDG
(*a*) s polarization; (*b*) p polarization. The order numbers are indicated below the corresponding curves

2.2. Direct Writing of Sub-micrometer DGs and Pattern Transfer

Surface-relief submicrometer DGs are realized in silicon. Positive PMMA e-beam resist with a thickness of $t = 200$ nm is spincoated on 3″ Si wafer with 100 nm top SiO_2 layer. Tests with variable shot exposure times are carried out to determine proper conditions to obtain near vertical profile and completely developing of the exposed resist. Reduction in e-beam shot size dshot in the designed linewidth was necessary to compensate the resist exposure from the backscattered electrons [18]. The determined optimal conditions are presented in Table 1. The resist is developed in mixture of methyl isobutyl ketone and isopropylalcohol.

Table 1. Exposure parameters

Λ (nm)	ξ	d_{shot} (nm)	d_{line} (nm)	τ (μs)
500	0.30	50	150	2800
600	0.33	50	200	2600
1000	0.40	250	400	1600

Plasma etching is performed on an Oxford Plasma Technology System 100 with ICP 180 source. The SiO_2 layer is etched in CHF_3 + Ar mixture using patterned PMMA as the masking layer. Just before etching post bake procedure has been carried out for 30 min at 100 °C to increase PMMA chemical resistance during the dry etching. The remained resist is stripped in chlorethylene and isopropylalcohol mixture. Relief with depth of 150 nm is etched in the silicon through the patterned SiO_2. The structures' sidewalls are prevented from undercutting by deposition of a polymer passivation layer. It is performed by adding a polymer forming gas into the plasma. The passivant must be anisotropically removed from the bottom of the trenches, achieved by the ion bombardment of the substrate. With gas chopping technique the polymer layer deposition and the process of its removal and silicon substrate etching are separated temporally. During the first step passivation is performed in CH_4 and CHF_3. At the time of the second step passivant is removed from bottom and Si is etched in a mixture of SF_6 and Ar. These two steps are repeated throughout the process [21]. Finally, SiO_2 is stripped in buffered HF. SEM pictures of the fabricated gratings are shown in Fig. 5.

The optical behaviour of the relief conductive DGs depends on a number of parameters: the material permittivity, the light polarization, the angle of incidence, the grating's thickness to wavelength ratio and period to wavelength ratio. Generally, maximum value of η_1 could be expected in Littrow configuration (occurring when the -1-th reflected order returns in the direction of the

incident beam) for p polarization and when the values of the wavelength, the period and the thickness are comparable [23, 24]. The mentioned above Littrow condition is satisfied when the angle of incidence is equal to $\theta_l = \arcsin \dfrac{\lambda}{2\Lambda}$. To exist diffraction orders λ must be smaller than 2Λ. Only one diffracted order exists in the described geometry until λ is greater than $2\Lambda/3$. The thick relief DGs exhibit high angular and spectral selectivity [20].

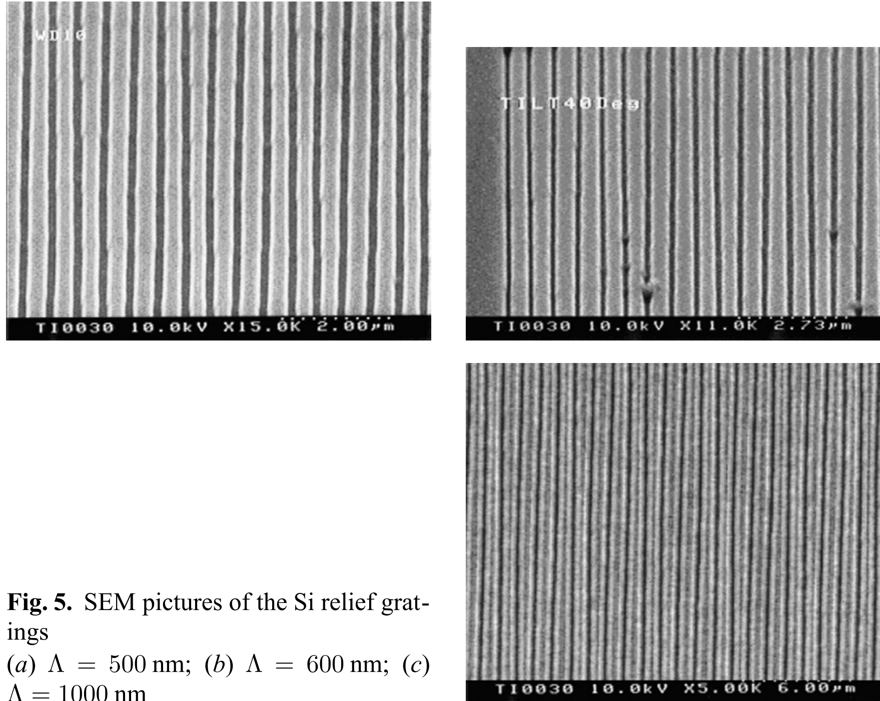

Fig. 5. SEM pictures of the Si relief gratings
(a) $\Lambda = 500$ nm; (b) $\Lambda = 600$ nm; (c) $\Lambda = 1000$ nm

Detailed investigation of the prepared DG is not the purpose of this work, because they are not optimized for given working conditions. The gratings DEs η_0 and η_1 are measured for p polarization in Littrow condition. The green and blue lines of an Ar laser are used for illumination. The spectral dependence of the quantity η_1/η_0, representing ratio of the energy in -1-st to that in 0-th order, is shown in Fig. 6. Densest DG shows strong maximum in the region when its period value is near the wavelength. The maximum in the η_1 for the other two gratings should be expected in the red and infrared region. The -1-st order DE could be increased by covering the gratings with metal with high reflectance in the working spectral region.

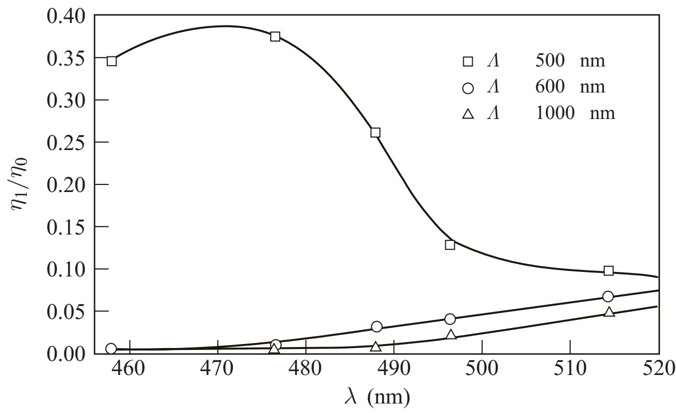

Fig. 6. Spectral dependence of the $\eta_1/|eta_0$

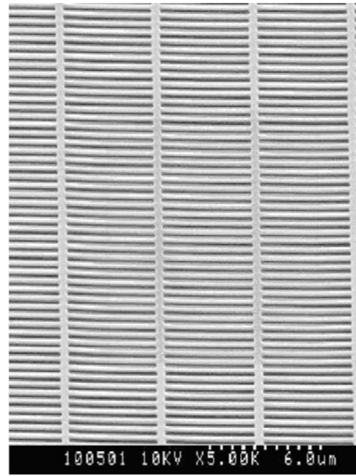

Fig. 7. Example of a 2D diffraction structure

In Figs 7 and 8 examples of 2 and 3 dimensional structures are presented. They are realized with the help of the direct e-beam writing on Si substrate with a spincoated PMMA resist. The grating from Fig. 7 represents regularly single shots array exposed in PMMA and developed. The periods in the picture directions are 0.8 and 5 μm. The optical diffraction pattern is result of the superposition of two orthogonal linear diffraction pictures. The angle of diffraction is different in the two directions because of the difference in the gratings periods. The structure of Fig. 8 is an example of deep RIE etching of Si. The technological step consequence is similar to that of submicrometer

period DGs except deeper RIE etching. The possibility to optimize the DE with the structure depth is an advantage of the described preparation technique.

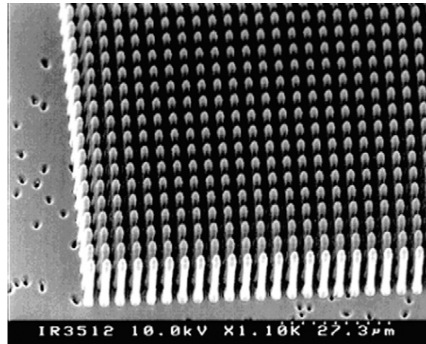

Fig. 8. Example of a 3D diffraction structure

3. Conclusion

E-beam lithography is used to fabricate different types of diffraction gratings and other regulary two-dimensional structures. Excellent quality binary chromium gratings are exposed on glass substrate. Designed periods are between 6 and 20 μm. Lines roughness and defect size are estimated of about 300 nm. The gratings optical behaviour is investigated in planar geometry and in TIR mode. Peculiarities in the DGs' diffraction efficiency are discussed. Relief DGs with periods between 0.5 and 1 μm are exposed and etched in silicon. Such gratings demonstrate high 1-st order DE in Littrow configuration. Small period gratings could be used as high selective and effective optical grids in the visible spectral region, as well as diffractive grids in UV and X-ray regions. The described preparation technique has the advantage of optimizing the grating's diffraction efficiency by changing the line depth. The results demonstrate the excellent possibilities of the e-beam lithography to fabricate structures for micro-fluidic applications with small dimensions and high requirements to the shape quality. It is a flexible alternative for realizing structures on non-planar surfaces or micro-fluidic channels. In combination with dry etching complicated 3-dimentional structures could be fabricated in "lab on a chip" technology.

The fabricated gratings are used as key constituent in design and fabrication of an miniaturised microfluidic TIR-DG sensor and a TIR based laser microrefractometer. In the latter the longitudinal lines binary DGs solve problem with automatic electronic detection of the diffraction orders disappearance in the laser microrefractometer construction, as well as with real time fluid temperature measurement. With the help of the prepared gratings an automatic working

microrefractometer prototype is constructed. The device is characterised with accuracy in the determined fluid's refractive index value better than 1×10^{-3}, easy operation, standard connection to a computer, compact size and possibility to perform measurements at different wavelengths [25]. The microrefractometer, as well as TIR-DG based sensor can be implemented in a "lab on a chip" sensor for investigating and analysis of the biomaterials, for medical diagnostic in-situ and in-vivo, etc.

Acknowledgements

This work was supported by Research Training Network contract No. HPRN-CT-1999-00150, WTZ project SVK 01/002 and grant VEGA 2/7185/20.

References

1. S. Sainov. Sens. Actuat. **45** (1994) 6.
2. Y. Sarov and S. Sainov. J. Opt. A: Pure and Appl. Optics **4** (2002) 382.
3. B. Anderson, A. Brodsky and L. Burgess. Anal. Chem **68** (1996) 1081.
4. A. Brodsky, L. Burgess and S. Smith. Appl. Spectr. **52** (1998) 332A.
5. S. Sainov and N. Dushkina. Appl. Opt. **29** (1990) 1406.
6. Y. Sarov, S. Shurulinkov and G. Minchev. Proceedings of SPIE **4397** (2000) 246.
7. B. Ioffe. *Refractometric Methods in Chemistry* (Chemistry, Leningrad, 1983).
8. K. Heuberger and W. Lukosz. Appl. Opt. **25** (1986) 1499.
9. K. Hill, B. Malo, F. Bilodeau, D. Johnson and J. Albert. Appl. Phys. Lett. **62** (1993) 1035.
10. G. Zhao, N. Tonge and J. Nishii. Jap. J. Appl. Phys. **37** (1998) 1842.
11. J. Zhang, K. Sugioka and K. Midorikawa. Opt. Lett. **23** (1998) 1486.
12. K. Kintaka, J. Nishii and N. Tohge. Appl. Opt, **39** (2000) 489.
13. E. Spasova, B. Mednikarov, G. Danev, S. Sainov and N. Dushkina. Proceedings of SPIE **1183** (1989) 683.
14. M. Josse and D. Kendall. Appl. Opt. **19** (1980) 72.
15. M. Wang and H. Su. Appl. Opt. **37** (1998) 7568.
16. B. Mednikarov, A. Poleshchuk and E. Churin. Optoelectr. Instrum. & Data Process **5** (1993) 82.
17. *Electron-beam Technology in Microelectronic Fabrication* (G. Brewer, Ed., Academic Press, New York 1980).
18. S. Saavedra and W. Reichert. Langmuir **7** (1991) 995.
19. *Handbook of Thin Film Technology* (L. Maissel and R. Brang, Eds, McGraw-Hill, New York 1970).
20. E. Loewen and E. Popov. *Diffraction Gratings and Applications* (Marcel Decher, New York 1997).
21. N. Dushkina and S. Sainov. J. Mod. Opt. **39** (1992) 173.
22. B. Volland, H. Heerlein, I. Kostic and I. Rangelow. Microelectronic Engineering **57–58** (2001) 641.

23. M. Moharam, T. Gaylord, G. Sincerbox, H. Werlich and B. Yung. Appl. Opt. **23** (1984) 3214.
24. M. Moharam and T. Gaylord. JOSA A **3** (1986) 1780.
25. Y. Sarov, I. Kostic, S. Minov, S. Mitkov, G. Minchev and L. Uher. *Automatic Laser Refractometer*, accepted in proceedings of SPIE.